Selection and Characterization of an RNA Decoy for Transcription Factor NF-κB†

Lori L. Lebruska and L. James Maher, III*

Department of Biochemistry and Molecular Biology, Mayo Foundation, Rochester, Minnesota 55905

Received October 21, 1998; Revised Manuscript Received January 4, 1999

ABSTRACT: Despite their chemical similarity, DNA and RNA sequences typically adopt very different structures within cells and are recognized by different proteins. However, a few interesting examples of proteins with dual specificity for DNA and RNA have previously been noted. These observations raise the possibility that RNA surrogates might be identified for many transcription factors that normally bind DNA. As an initial test of this novel concept, we used in vitro selection to isolate a small RNA aptamer that binds with nanomolar affinity to human transcription factor NF-κB, a key regulator of inflammation, HIV-1 gene expression, and apoptosis. Selected RNAs contain a 31-nucleotide core domain that was shown by mutation and deletion analyses to be necessary and sufficient for NF-κB binding. Neither DNA nor 2′-*O*-methyl RNA analogues of the aptamer bound NF-κB. The results of competition experiments demonstrate that binding of the RNA aptamer blocks the ability of NF-κB to bind duplex DNA. Expression of this aptamer structure within heterologous nuclear RNA transcripts may provide a new strategy to inhibit NF-κB function in vivo. Aptamers that inhibit transcription factors might be useful in a variety of applications.

In vitro selection has been used to identify high-affinity RNA aptamers specific for a variety of small and large molecules (*1*−*11*). We wondered whether in vitro selection could be used to identify RNA aptamers that bind tightly to transcription factors. In principle, such RNAs might compete with DNA for transcription factor binding, offering a novel strategy for the inactivation of these proteins. We approached this problem by attempting to select RNA aptamers specific for human transcription factor NF-κB.

First identified for its role in immunoglobulin expression (*12*), human NF-κB is a DNA-binding heterodimer of p65 and p50 subunits (p50/p65), homologous to the *rel* protooncogene family of proteins. NF-κB is also found as a p50 homodimer ($p50_2$) that bind to similar sites in duplex DNA (e.g., 5′-GGGACTTTCC; *13*). High-resolution structures of $p50_2$ and p50/p65 bound to DNA have been determined by X-ray crystallography (*14*, *15*). Although both $p50_2$ and p50/p65 bind similar κB sites, $p50_2$ activates transcription through distinct mechanisms because, unlike p65, p50 lacks a potent carboxy-terminal transcriptional activation domain. Thus, p50 and p65 homo- or heterodimers activate transcription from different κB sites in a sequence- and context-dependent manner (*16*).

NF-κB is an important activator of genes involved in immune functions such as inflammation and the synthesis of chemokines, interferons, MHC proteins, growth factors, and cell adhesion molecules (*17*). NF-κB activation is also required for HIV-1 gene expression due to the presence of two essential κB binding sites in the viral long terminal repeat (LTR). Inactive NF-κB protein is present in the cytoplasm complexed with an inhibitory subunit, I-κB. NF-κB is activated by several modalities including tumor necrosis factor (TNF)[1] and ultraviolet light (*17*). During activation, I-κB in the NF-κB/I-κB complex is degraded by proteolysis after phosphorylation and ubiquitination. Once free from the inhibitory subunit, NF-κB is transported to the nucleus and activates target gene expression.

Inhibition of NF-κB-dependent gene activation could be a valuable strategy for enhancing the activities of antiviral and anticancer agents. Inhibition of induced NF-κB has been shown to potentiate tumor cell killing by tumor necrosis factor (TNF), anticancer drugs, and radiation (*18*). Furthermore, NF-κB activation suppresses the ability of oncogenic *ras* mutations to stimulate apoptosis in tumor cells (*19*). The potential practical value of inhibiting NF-κB in tumor cells has been suggested by the antitumor activities of antisense oligonucleotides targeting NF-κB in tissue culture and animal models (*20*, *21*).

Besides antisense approaches, several strategies can be imagined for artificial inhibition of NF-κB. Small molecule inhibitors of I-κB kinase are plausible targets, together with other compounds that interfere with I-κB processing and degradation. These approaches would prevent nuclear import of active NF-κB protein. A complementary strategy involves compounds that prevent activated nuclear NF-κB from gaining access to its target κB sites in genomic DNA. One approach involves identification of soluble molecular decoys that could act as surrogates for NF-κB binding sites in duplex DNA.

† This work was supported by the Mayo Foundation, by NIH Grants GM47814 and GM54411, and by a Siebens Foundation Grant in Molecular Medicine. L.J.M. is a Harold W. Siebens Research Scholar. L.L.L. is supported by NRSA Fellowship GM20070.

* To whom correspondence should be addressed at the Department of Biochemistry and Molecular Biology, Guggenheim 16, Mayo Foundation, 200 First St., S.W., Rochester, MN 55905. Phone: 507-284-9041. Fax: 507-284-2053. E-mail: maher@mayo.edu.

[1] Abbreviations: TNF, tumor necrosis factor; nt, nucleotide(s); HEPES, 4-(2-hydroxyethyl)-1-piperazineethanesulfonic acid; EDTA, ethylenediaminetetraacetic acid; DTT, dithiothreitol; PMSF, phenylmethylsulfonyl fluoride; SDS, sodium dodecyl sulfate; SB, selection buffer; MMLV, Maloney murine leukemia virus; TBE, Tris−borate, EDTA.

10.1021/bi982515x CCC: $18.00 © 1999 American Chemical Society
Published on Web 02/13/1999

An obvious candidate for an NF-κB molecular decoy is a phosphorothioate-modified duplex DNA copy of the κB target site itself. This approach was successfully used to inhibit NF-κB-dependent gene expression in cell culture (*22*), and has been applied in several experimental systems (*23, 24*). Despite its simplicity and appeal, inhibition by DNA decoys requires a continuous source of the exogenous DNA, together with the need to deliver these molecules to target cell nuclei. Improvements in nuclear delivery of duplex DNA oligonucleotides and analogues are required to facilitate this technique.

On the other hand, we have been intrigued by the concept that RNA aptamers might be selected from combinatorial libraries to bind with high affinity to transcription factors such as NF-κB. Unlike DNA, RNA transcripts containing such aptamers might be expressed under regulated control from a transgene in the nucleus of the target cell. In this way, the therapeutic RNA macromolecule would be encoded and produced in the nucleus.

We have chosen to seek novel RNA inhibitors of NF-κB using in vitro genetic selections from random RNA libraries containing $\sim 10^{14}$ RNAs. Each member of the library is a 100-nucleotide (nt) RNA, in which 60 nt are randomized. Novel RNAs capable of binding specifically to a variety of classes of target molecules have previously been identified using this approach (*1*−*3*, *6*, *25*). We show that a high-affinity RNA ligand for a DNA binding transcription factor can be identified, and that the RNA ligand competes with DNA for transcription factor binding. The inherently favorable electrostatic character of the DNA binding site may make this location attractive for RNA aptamers during selection.

MATERIALS AND METHODS

Oligonucleotides. DNA oligonucleotides were synthesized by phosphoramidite methodology using an Applied Biosystems Model 380B DNA synthesizer. RNA oligonucleotides were synthesized using appropriately protected RNA phosphoramidites followed by the methylamine deprotection protocol suggested by the supplier (Glen Research, Sterling, VA). 2′-*O*-Methyl oligonucleotides were synthesized with monomers obtained from Glen Research. Molecular masses of synthetic oligonucleotides were confirmed by electrospray ionization mass spectroscopy in the negative ion mode after on-line cation exchange to suppress metal adducts. Synthetic DNA templates for the selection pool were of the form 5′ $A_5TATG_2A_2CGCT_2CATGCAT$-[$N_{60}$]-$CTCGAG_2ATATC_3$-TATAGTG where N indicates any base. Nucleotides in the random region were synthesized from a mixture of phosphoramidites adjusted for the relative coupling efficiency of each monomer. Primers used for reverse transcription and/or PCR amplification of the DNA pool were 5′ TA_2TAC-GACTCACTATAG$_3$ATATC$_2$TCGAG and 5′ A_5TATG_2-$ACGCT_2CATGCAT$.

Duplex DNA targets used in electrophoretic mobility shift assays were prepared by annealing complementary strands in a 1:1 ratio in the presence of 200 mM NaCl. Duplex DNA was radiolabeled using the Klenow fragment of DNA polymerase I by filling in recessed 3′ termini with [α-^{32}P]-dATP in the presence of 2 mM each dGTP, dTTP, and dCTP.

Protein Expression and Purification. A plasmid encoding human p50 (*14*) was transformed into *E. coli* strain BL21-(DE3). One liter of bacterial culture was induced at $A_{600} = 0.2$ with 0.2 mM IPTG at 37 °C. At $A_{600} = 0.6$, cells were

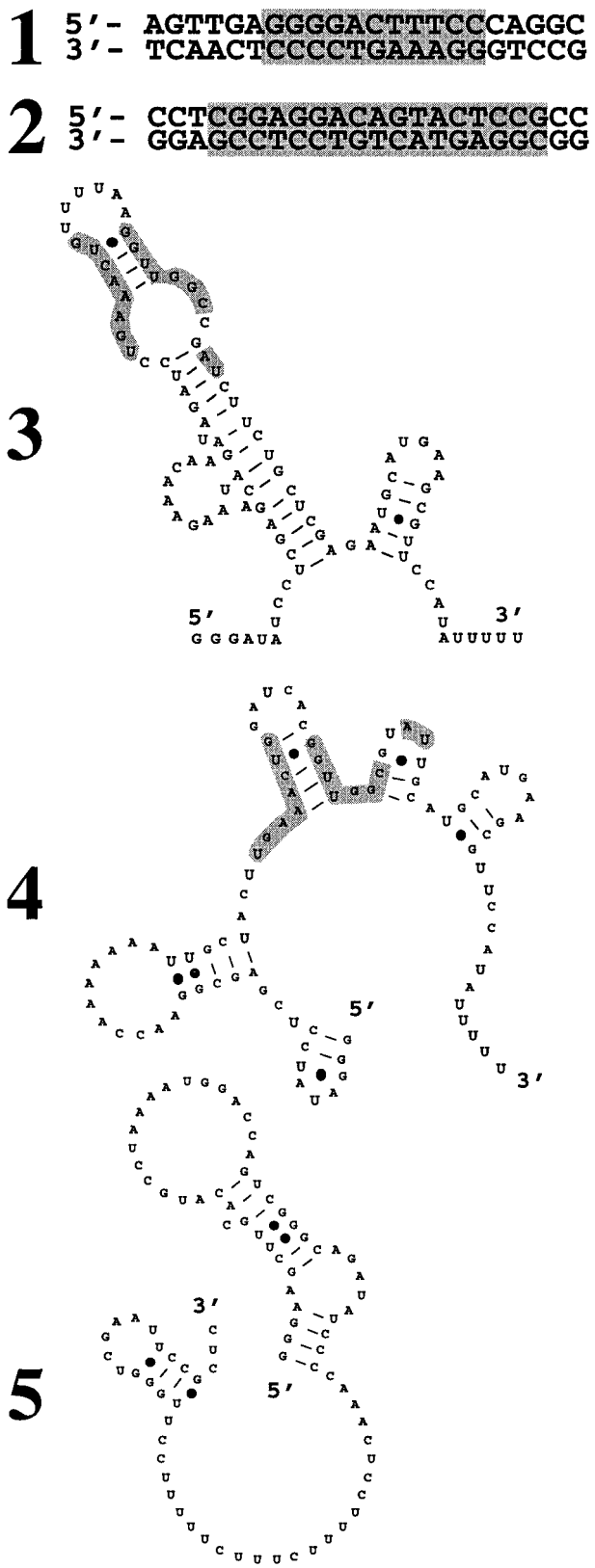

FIGURE 1: Experimental nucleic acids. Synthetic DNA duplexes contained the κB binding site (DNA duplex **1**) or the GAL4 binding site (DNA duplex **2**). The respective protein binding sites are shaded. RNA aptamers **3** (98 nt) and **4** (88 nt) were selected in vitro and are depicted according to the predictions of an RNA folding algorithm. Sequences shared by RNAs **3** and **4** are shaded. RNA **5** is a nonspecific sequence of similar length.

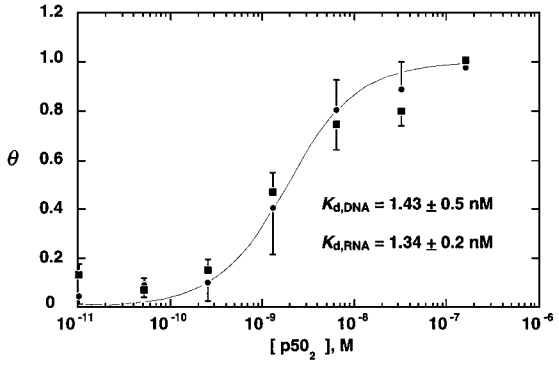

FIGURE 2: Estimation of equilibrium dissociation constants for $p50_2$ binding to DNA duplex **1** and RNA aptamer **3**. Nitrocellulose filter binding assays were performed with radiolabeled duplex **1** (1.4 nM) or radiolabeled RNA aptamer **3** (0.9 nM) in the presence of increasing concentrations of $p50_2$ protein. The fractional saturation of the radiolabeled probe (θ) is plotted as a function of protein concentration for the DNA duplex (■) or RNA aptamer (●). Error bars indicate standard deviation. The indicated equilibrium dissociation constant estimates were determined by curve fitting to eq 1 as described under Materials and Methods.

harvested, washed, and frozen. Pellets were then resuspended in 30 mL of buffer A (20 mM HEPES, pH 7.5, 0.4 M NaCl, 2 mM EDTA, 5% v/v glycerol, 1 mM DTT, 0.5 mM PMSF, 1 μg/mL pepstatin, 1 μg/mL leupeptin) and sonicated. Cell debris was pelleted, and 10% w/v polyethyleneimine was added to precipitate nucleic acids. Saturated ammonium sulfate was added to 55% w/v, and precipitated protein was collected by centrifugation. The resulting pellet was dissolved in 50 mL of buffer B (20 mM HEPES, pH 7.5, 2 mM EDTA, 5% v/v glycerol, 1 mM DTT, 0.5 mM PMSF, 1 μg/mL pepstatin, 1 μg/mL leupeptin) and loaded onto a Hi trap-sepharose column which was washed and then developed with a NaCl gradient. Fractions were checked by SDS gel electrophoresis. Peak fractions were pooled and chromatographed over a Superdex-200 size exclusion column (Pharmacia, 10 000−600 000 range) and peak fractions concentrated to 1 mL. The purified protein was stored in buffered 50% glycerol at −20 °C.

Selection of RNAs That Bind to p50₂. The initial pool of random RNAs was prepared by PCR amplification and in vitro transcription as described (*9*). The initial selection involved ~366 pmol of RNA library (~2 transcripts each from ~10^{14} initial DNA templates). RNAs were preincubated with 0.2 μm nitrocellulose filter strips in 0.5 mL of selection buffer (SB: 10 mM HEPES, pH 7.5, 0.1 M NaCl, 1 mM DTT) to preabsorb RNAs with high affinity for nitrocellulose. RNAs were then diluted to 1.5 nM in SB and incubated with 0.24 nM $p50_2$ in a volume of 250 mL for 2 h with mild agitation at 37 °C. This RNA concentration was chosen to reduce the initial fraction of labeled RNA bound by $p50_2$ to below 1%. Mock reactions without $p50_2$ were performed in parallel. Binding reactions were filtered through nitrocellulose membranes premoistened with SB, followed by washing with 5 mL of SB. Bound RNAs were then eluted by incubating filters in 0.5 mL of elution buffer (200 mM Tris-HCl, pH 7.6, 2.5 mM EDTA, 300 mM NaCl, 2% SDS) at 65 °C for 35 min. The resulting solution was extracted with an equal volume of phenol/chloroform (1:1) and precipitated with ethanol. Half of the selected RNA was reverse-transcribed using the appropriate primer and MMLV reverse transcriptase as described (*9*). Recovery of selected radiolabeled RNA at each round was monitored by Cerenkov counting.

Cloning and Sequencing. Double-stranded DNA products amplified after various rounds were cloned using the pGEM-T Vector System I (Promega) and sequenced in the Mayo Foundation Molecular Biology Core Facility. Predicted RNA secondary structures were determined using the program Mulfold (*26*−*28*).

Affinity Determination. Data to estimate the K_d for binding of $p50_2$ to radiolabeled DNA duplex **1** (1.4 nM; Figure 1) or radiolabeled RNA aptamer **3** (0.9 nM; Figure 1) were obtained by incubation with decreasing amounts of $p50_2$ (161 nM to 10.4 pM) in SB and filtering the reaction over nitrocellulose membranes prewetted in SB. Protein-bound RNAs were quantitated by Cerenkov counting. K_d values were estimated by measuring the fractional saturation (θ) of the radiolabeled nucleic acid target (*T*) as a function of the concentration of added $p50_2$ protein (*P*) and fitting to the equation:

$$\theta = \frac{1}{2[\mathrm{T}]_t}[[\mathrm{T}]_t + K_d + [\mathrm{P}]_t - \sqrt{([\mathrm{T}]_t + K_d + [\mathrm{P}]_t)^2 - 4[\mathrm{P}]_t[\mathrm{T}]_t}] \quad (1)$$

where the subscript (t) refers to total concentration, and it need not be assumed that $[\mathrm{P}]_t \sim [\mathrm{P}]_{free}$. Curve fitting was performed with Kaleidagraph software.

Electrophoretic Mobility Shift Experiments. The ability of various nucleic acids to block protein binding to κB sites was measured in competition experiments which included radiolabeled DNA duplex **1** (0.6 nM) and 1−8-fold molar excess (relative to labeled probe) of the indicated competitor RNA or DNA. Ten microliter binding reactions contained 1 μg of poly(dI·dC), 10 mM HEPES, pH 7.5, 0.1 M NaCl, and 1 mM DTT. Protein ($p50_2$; 0.3 nM) was then added, followed by incubation for 5 min at ambient temperature

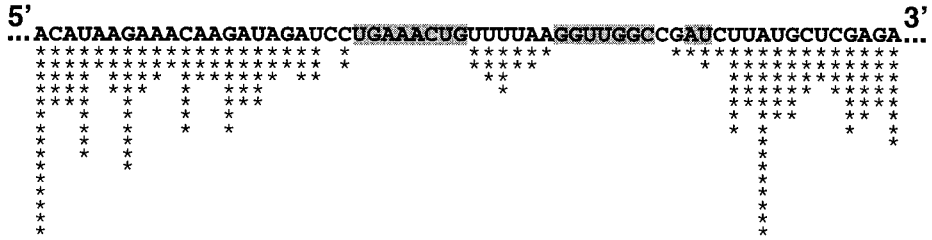

FIGURE 3: Partial rerandomization of RNA aptamer **3** to identify sequences important for $p50_2$ binding. A degenerate pool of **3**-like RNAs was subjected to additional cycles of selection for binding to $p50_2$. Shading indicates nucleotides shared between RNA aptamers **3** and **4**. Mutations compatible with $p50_2$ binding are indicated (asterisks).

and electrophoresis through native polyacrylamide gels in 0.5 × TBE buffer. Complexes were detected and analyzed by storage phosphor technology.

Boundary Determination. RNAs were transcribed in vitro and purified as described above. RNAs were treated with alkaline phosphatase and then radiolabeled at their 5′ termini using T4 polynucleotide kinase (*29*). Alternatively, RNAs were labeled at their 3′ termini using [α-^{32}P]pCp (Amersham) and T4 RNA ligase (*30*). Labeled RNAs were purified by denaturing polyacrylamide gel electrophoresis and subjected to partial T_1 RNase digestion to map G residues, or partial alkaline hydrolysis with 50 mM Na_2HCO_3 (pH 9.4) as described (*31*). After partial alkaline hydrolysis, RNA fragments competent to bind $p50_2$ were selected in binding reactions containing SB, 1 μg of poly(dI·dC), and 5×10^{-7} M $p50_2$. After incubation at 37 °C for 5 min, binding reactions were filtered over nitrocellulose filters. The filters were washed, and bound RNAs were eluted and precipitated as previously described. RNA samples were analyzed by electrophoresis through 8% denaturing polyacrylamide sequencing gels containing 7.5 M urea.

RESULTS AND DISCUSSION

A High-Affinity RNA Ligand for $p50_2$. Recombinant $p50_2$ protein (*14*) was overexpressed and purified from *E. coli* for in vitro selection experiments. In preliminary experiments (data not shown), purified $p50_2$ exhibited specific binding to DNA duplex **1** containing a κB binding site, but not to DNA duplex **2** containing a GAL4 binding site (Figure 1). We identified RNA aptamers capable of tightly binding $p50_2$ using cycles of in vitro affinity selection and amplification (*1, 2*). The initial RNA pool represented ~10^{14} different sequences consisting of a core of 60 random nucleotides flanked by fixed sequences for reverse transcription and PCR (*9*). Low RNA concentrations (<1.5 nM) were required to limit binding of the random RNA pool to less than 1% in initial rounds. This was achieved by performing selections in large volumes (250 mL). Fourteen cycles of selection and amplification were performed after which a dominant RNA was detected as 21 of 26 cloned and sequenced cDNAs (RNA aptamer **3** in Figure 1). A related RNA, aptamer **4** (Figure 1), appeared in 3 of the 26 cloned sequences. The two remaining cloned sequences appeared to be unrelated (data not shown). A region of sequence similarity was present in RNA aptamers **3** and **4** (shaded in Figure 1). When folded according to a free energy minimization method (*26*−*28*), these similar nucleotides formed a short stem−loop structure. RNA aptamer **3** was selected for further study.

Equilibrium dissociation constants for RNA aptamer **3** and duplex DNA **1** binding to $p50_2$ were estimated using nitrocellulose filter binding assays (Figure 2). Remarkably, the measured dissociation constant for $p50_2$ binding to RNA aptamer **3** (~1 nM) was similar to that measured for DNA duplex **1**. The high binding affinity of the selected RNA aptamer **3** for $p50_2$ was striking, and raised the possibility that RNA aptamer **3** might competitively inhibit the binding of $p50_2$ to its natural DNA target.

Essential Nucleotides for RNA Aptamer 3 Binding to $p50_2$. To identify nucleotides essential for RNA aptamer **3** to interact with $p50_2$, the aptamer was retranscribed from a moderately degenerate DNA template such that the "correct" residue of RNA aptamer **3** was encoded at each position with a probability of 0.7. Each of the three possible "incorrect"

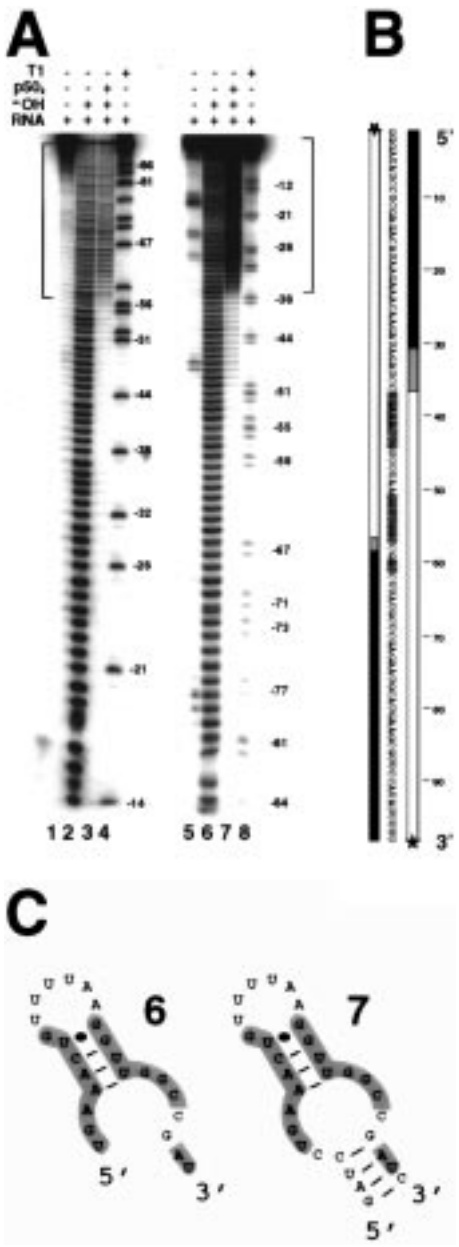

FIGURE 4: Mapping the boundaries of RNA aptamer **3** essential for $p50_2$ binding. (A) RNA aptamer **3** (5′ radiolabeled in lanes 1−4; 3′ radiolabeled in lanes 5−8) was partially hydrolyzed with alkali, and fragments were incubated in the presence of $p50_2$. Labeled RNA fragments competent to bind $p50_2$ were collected on nitrocellulose filters. RNA was eluted from the filters followed by denaturing gel electrophoresis as described under Materials and Methods: untreated RNA (lanes 1 and 5); RNA fragments resulting from alkaline hydrolysis (lanes 2 and 6); RNA fragments competent to bind $p50_2$ (lanes 3 and 7); RNA treated with RNase T_1 (lanes 4 and 8). Brackets indicate RNA fragments competent for $p50_2$ binding. (B) Summary of boundary experiment results. Stars indicate the positions of radiolabels in the two experiments. Regions where strand breaks gave rise to labeled RNA fragments that bound $p50_2$ strongly (black boxes), weakly (gray boxes), or not at all (white boxes) are shown. RNA sequence shading indicates nucleotides shared between RNAs **3** and **4**. (C) Derivatives of RNA aptamer **3** tested for binding activity. RNA aptamer **6** (25 nt) is based on the minimal predictions of data in Figures 2 and 3. RNA aptamer **7** (31 nt) is a slightly longer derivative. The indicated RNA secondary structures were predicted by a folding algorithm.

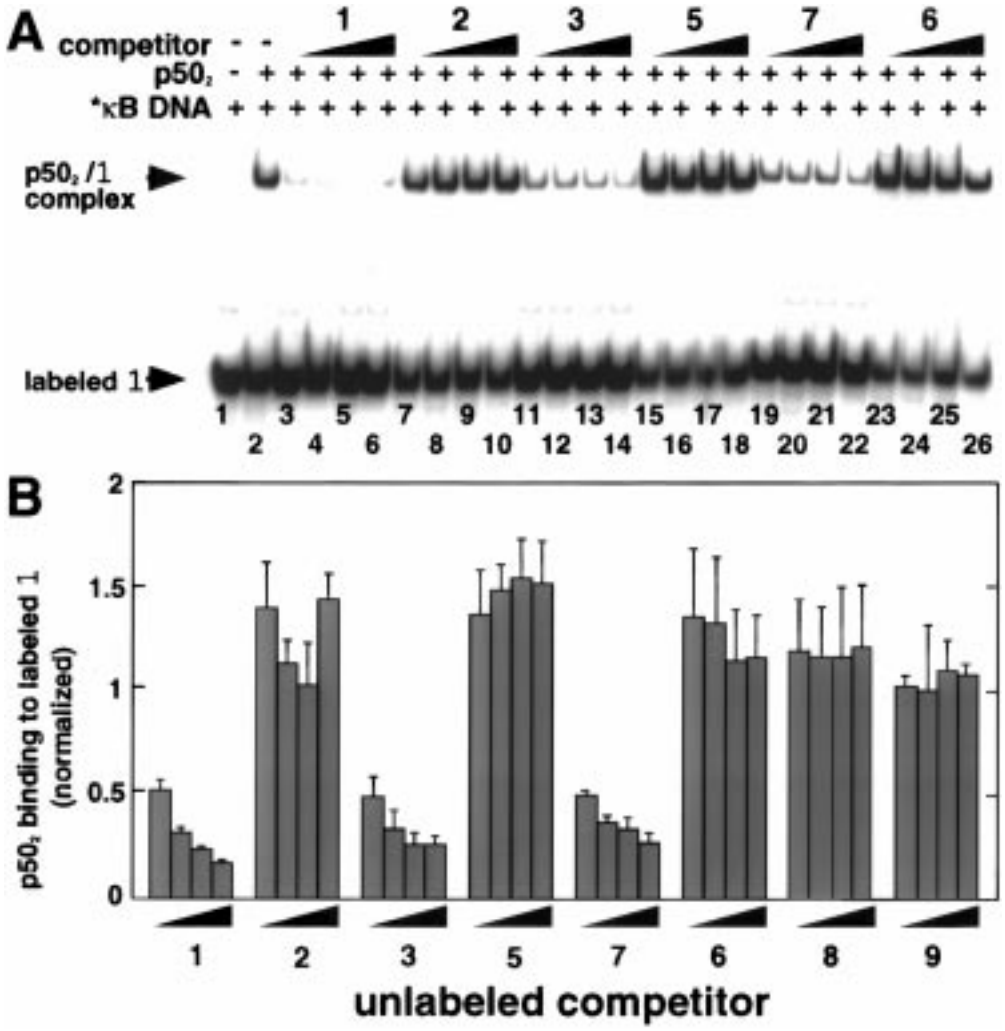

FIGURE 5: Selected RNA aptamers compete with duplex DNA for binding to $p50_2$. Labeled DNA duplex **1** was incubated in the absence of protein (lane 1) or in the presence of $p50_2$ alone (lane 2) or together with various unlabeled competitors (lanes 3−26): unlabeled DNA duplex **1** (lanes 3−6), DNA duplex **2** (lanes 7−10), RNA aptamer **3** (lanes 11−14), nonspecific RNA **5** (lanes 15−18), RNA aptamer **6** (lanes 19−22), or RNA aptamer **7** (lanes 23−26). Triangles indicate increasing unlabeled competitor concentration (1-, 2-, 4-, or 8-fold molar excess relative to radiolabeled DNA duplex **1**). Experiments were performed such that radiolabeled DNA duplex **1** was in excess over $p50_2$. (B) Quantitation of competitive inhibition of DNA binding. Error bars reflect standard deviation from 3 independent experiments. Binding data are presented as values of θ relative to the level of radiolabeled DNA duplex **1** binding in the absence of competitor.

residues was encoded at each position with a probability of 0.1. Four additional rounds of in vitro selection for $p50_2$ binding were then performed with the degenerate RNA library. Representative clones were sequenced. Point mutations compatible with $p50_2$ binding are shown in Figure 3. Two regions intolerant of mutations were observed. These regions correspond closely to sequences shared between selected RNA aptamers **3** and **4** (Figure 1), suggesting that they represent the functional RNA domain for $p50_2$ binding.

To corroborate these data, an RNA boundary experiment was performed wherein the $p50_2$ binding competence of successive 5′ or 3′ deletion variants of RNA aptamer **3** was assessed (Figure 4). 5′ (Figure 4A, lanes 1−4) or 3′ (Figure 4A, lanes 5−8) end-labeled RNAs were subjected to partial alkaline hydrolysis (Figure 4A, lanes 2 and 6) to create a population of random end-labeled fragments. Nitrocellulose filter binding assays were used to select fragments competent to bind $p50_2$ (Figure 4A, lanes 3 and 7). 5′ end-labeled RNAs as short as 61 nt retained the ability to bind $p50_2$ as did 3′ end-labeled RNAs as short as 31 nt. Intermediate levels of $p50_2$ binding were observed as RNA length decreased over 2−6 nt from either terminus. Shorter RNAs did not detectably bind $p50_2$. The minimum active domain of RNA aptamer **3** defined by these boundary experiments again comprised approximately the nucleotide sequence shared between selected RNA aptamers **3** and **4** (Figure 4B).

RNA Aptamers as "Decoys" for NF-κB. To confirm the minimal RNA aptamer domain required for $p50_2$ binding, RNA oligonucleotides **6** and **7** were chemically synthesized (Figure 4C). RNA oligonucleotide **6** corresponds to the minimal RNA domain suggested by boundary and mutagenesis studies, whereas RNA oligonucleotide **7** was prepared to conserve the adjacent stem region in the predicted folded structures of the aptamer.

We considered the possibility that RNA aptamers selected for tight binding to $p50_2$ might interact with basic amino acid residues lining the DNA recognition surface of the protein (*14*). Such RNAs might therefore compete with DNA duplex **1** for $p50_2$ binding. To test this hypothesis, we monitored the ability of unlabeled RNA aptamer **3** and RNA oligonucleotides **6** and **7** to compete with radiolabeled DNA duplex **1** for $p50_2$ binding in gel mobility shift assays.

Binding experiments were performed with radiolabeled DNA duplex **1** in excess over $p50_2$, together with the indicated molar excess of unlabeled competitor DNA or RNA relative to labeled DNA duplex **1** (Figure 5A). Competition was observed in the presence of excess unlabeled DNA duplex **1**, as expected (Figure 5A, lanes 3−6). Moreover, unlabeled DNA duplex **2** was unable to compete for $p50_2$ (Figure 5A, lanes 7−10). Strikingly, unlabeled RNA aptamer **3** effectively competed with radiolabeled DNA duplex **1** for $p50_2$ binding (Figure 5A, lanes 11−14), while irrelevant RNA **5** did not compete for $p50_2$ binding (Figure 5A, lanes 15−18). Short RNA oligonucleotides **6** and **7** differed in their ability to compete with radiolabeled DNA duplex **1** for $p50_2$ binding. RNA **6** (25 nt) failed to compete for $p50_2$ binding (Figure 5A, lanes 23−26), whereas RNA **7** (31 nt) was as effective a molecular decoy as unlabeled DNA duplex **1** or full-length RNA aptamer **3** (Figure 5A, lanes 19−22). This result points to the possible significance of a stem structure in properly configuring the RNA aptamer for $p50_2$ binding (Figure 4C).

In experiments to determine if the selected RNA aptamer specificity is specific for NF-κB, excess unlabeled RNA **7** did not inhibit the binding of recombinant GAL4 transcription factors to the GAL4 recognition site in DNA duplex **2** (data not shown).

The short length of RNA **7** (31 nt) suggested that potentially useful nucleic acid analogues of RNA **7** might also bind $p50_2$. Therefore, DNA and 2′-*O*-methyl analogues of RNA **7** were prepared. However, neither DNA **8** nor 2′-*O*-methyl RNA **9** displayed decoy activity (Figure 5B), suggesting that at least one 2′-hydroxyl group in RNA aptamer **7** is essential for $p50_2$ binding.

Having performed selections using truncated recombinant $p50_2$ (amino acids 40−366), we addressed the ability of RNA aptamer **7** to bind to a full-length recombinant form of $p50_2$ (amino acids 1−504), as well as to a recombinant form of the transcriptionally active heterodimer composed of p50/p65 subunits. These proteins were expressed in a baculovirus system (*32*), and RNA aptamer binding was assessed in gel shift competition assays (Figure 6). As previously observed for $p50_2$, RNA aptamer **7** competed with radiolabeled DNA duplex **1** for binding to full-length $p50_2$ (Figure 6A), whereas only modest competition was seen with unlabeled DNA duplex **2** or RNA **6** (Figure 6A). Similar results were obtained for the p50/p65 form of NF-κB (Figure 6B). These data show that RNA aptamer **7** is competent to bind both $p50_2$ and p50/p65 forms of NF-κB, and creates complexes with each protein that block binding to DNA. In a formal sense, RNA aptamer **7** thus behaves as a molecular decoy for NF-κB.

To explore the possibility that RNA aptamers **3** and **7** block NF-κB binding to DNA by disrupting protein dimerization, gel mobilities of protein complexes with radiolabeled DNA duplex **1** vs radiolabeled RNA aptamer **7** were compared. These complexes comigrated on native polyacrylamide gels, suggesting that both involve dimeric forms of p50 (data not shown).

Natural Examples. The premise that a folded RNA can serve as a decoy to block transcription factor binding to DNA has a natural precedent in the apparent autoregulation of 5S rRNA transcription in *Xenopus*, a process that is likely to occur in all metazoans (*33*). TFIIIA is a zinc finger-containing transcription factor that binds and activates the 5S rRNA gene for transcription by RNA polymerase III (*33*). Remarkably, the resulting 5S rRNA transcript can also bind to TFIIIA with high affinity, thus competing with its own promoter DNA for TFIIIA (*33*). The result is autogenous feedback control with 5S rRNA serving as a "decoy" for its own transcription factor.

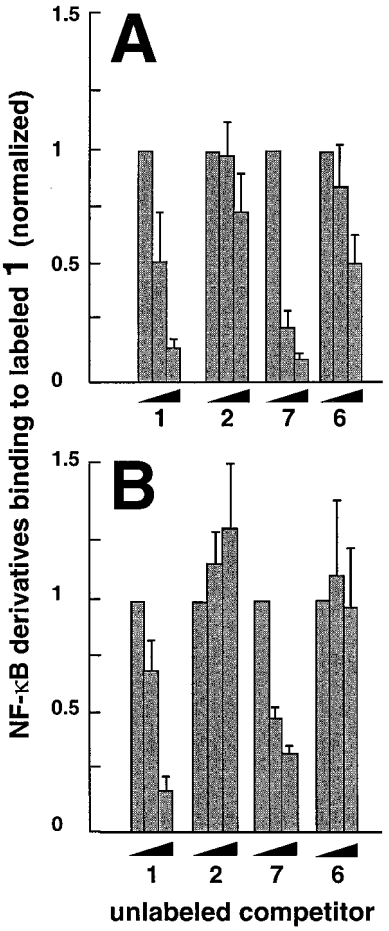

FIGURE 6: Competition of RNA aptamer **7** for binding to $p50_2$ or p50/p65 forms of NF-κB in the presence of radiolabeled DNA duplex **1**. (A) Recombinant, full-length $p50_2$ was incubated in the presence of radiolabeled DNA duplex **1** and the indicated unlabeled competitors. Binding was analyzed as in Figure 5. Triangles indicate increasing unlabeled competitor concentration (0-, 1-, or 5-fold molar excess relative to radiolabeled DNA duplex **1**). Experiments were performed under conditions such that radiolabeled DNA duplex **1** was in excess over the NF-κB protein derivative. (B) Recombinant p50/p65 (NF-κB) was incubated in the presence of radiolabeled DNA duplex **1** and the indicated unlabeled competitors.

Recently, it has been shown that the *Drosophila* homeodomain transcription factor bicoid is also capable of binding to both DNA and RNA (*34, 35*). Bicoid forms an anterior-to-posterior concentration gradient in the *Drosophila* embryo and activates several segmentation genes. Where present in high concentrations, bicoid binds sequence-specifically to the 3′ UTR of the mRNA encoding the caudal transcription factor, which suppresses its translation. Thus, zinc finger and homeodomain transcription factors have been found that bind to both DNA and RNA. These discoveries suggest that RNA binding to transcription factors may be an important natural mode of gene regulation. The aptamer identified in the present experiments might recapitulate an RNA structure that

also occurs naturally representing an as yet undescribed target for NF-κB regulation.

Future Prospects. The significant roles of the p50/p65 form of NF-κB in regulation of inflammation (*17*), apoptosis (*36*), and HIV-1 replication (*37*) have made this molecule an interesting target for design of therapeutic inhibitors. Previous approaches have relied on antisense agents against p65 (*20, 21*), or phosphorothioate analogues of κB sites in duplex DNA (*23, 24*). These strategies would require continuous exogenous administration of oligonucleotide-based compounds, known to be poorly targeted to cell nuclei. Transgene-based approaches have included transfection of target cells with dominant negative forms of I-κB (*38*). An advantage of such approaches is that gene transfer allows the inducible delivery of an inhibitor from within the target cell. Moreover, whereas DNA-based decoys for NF-κB cannot be produced endogenously, decoy RNA aptamers such as those described here might be produced in the target cell nucleus after gene transfer. When synthesized at appropriate levels, RNA transcripts carrying such aptamers might function to modify inflammatory responses, to hasten apoptosis, or to reduce HIV-1 transcription.

ACKNOWLEDGMENT

We thank G. Soukup, L. Tomky, M. Ferber, and other past and present members of the Maher laboratory. We acknowledge G. Verdine, R. Chopra, C. Rosen, T. Coleman, T. Wiegand, C. Paya, and D. Burke for providing materials and advice, and S. Strobel and S. Russell for comments on the manuscript. We appreciate excellent assistance from staff of the Mayo Foundation Molecular Biology Core Facility (M. Doerge), Protein Core Facility (C. Charlesworth), Biological Mass Spectrometry Core Facility (S. Naylor, A. Tomlinson, and L. Benson), and Biomathematics Core Facility (Z. Bajzer).

REFERENCES

1. Tuerk, C., and Gold, L. (1990) *Science 249*, 505−510.
2. Ellington, A. D., and Szostak, J. W. (1990) *Nature 346*, 818−822.
3. Tuerk, C., MacDougal, S., and Gold, L. (1992) *Proc. Natl. Acad. Sci. U.S.A. 89*, 6988−6992.
4. Gold, L. (1995) *J. Biol. Chem. 270*, 13581−13584.
5. Binkley, J., Allen, P., Brown, D. M., Green, L., Tuerk, C., and Gold, L. (1995) *Nucleic Acids Res. 23*, 3198−3205.
6. Nieuwlandt, D., Wecker, M., and Gold, L. (1995) *Biochemistry 34*, 5651−5659.
7. Abelson, J. N. (1996) in *Methods in Enzymology*, Academic Press, New York.
8. Burke, D., Scates, L., and Andrews, K. (1996) *J. Mol. Biol. 264*, 650−666.
9. Soukup, G. A., Ellington, A. D., and Maher, L. J. (1996) *J. Mol. Biol. 259*, 216−228.
10. Gold, L., Brown, D., He, Y.-Y., Shtatland, T., Singer, B. S., and Wu, Y. (1997) *Proc. Natl. Acad. Sci. U.S.A. 94*, 59−64.
11. Yoo, S., and Dynan, W. S. (1998) *Biochemistry 37*, 1336−1343.
12. Sen, R., and Baltimore, D. (1986) *Cell 46*, 705.
13. Kunsch, C., Ruben, S. M., and Rosen, C. A. (1992) *Mol. Cell. Biol. 12*, 4412−4421.
14. Muller, C. W., Rey, F. A., Sodeoka, M., Verdine, G. L., and Harrison, S. C. (1995) *Nature 373*, 311−317.
15. Chen, F. E., Huang, D.-B., Chen, Y.-Q., and Gosh, G. (1998) *Nature 391*, 410−413.
16. Fujita, T., Nolan, G. P., Ghosh, S., and Baltimore, D. (1992) *Genes Dev. 6*, 775−787.
17. Verma, I. M., Stevenson, J. K., Schwarz, E. M., Antwerp, D. V., and Miyamoto, S. (1995) *Genes Dev. 9*, 2723−2735.
18. Beg, A. A., and Baltimore, D. (1996) *Science 274*, 782−784.
19. Mayo, M. W., Wang, C.-Y., Cogswell, P. C., Rogers-Graham, K. S., Lowe, S. W., Der, C. J., and Baldwin, A. S. (1997) *Science 278*, 1812−1815.
20. Kitajima, I., Shinohara, T., Bilakovics, J., Brown, D. A., Xu, X., and Nerenberg, M. (1992) *Science 258*, 1972−1795.
21. Higgins, K. A., Perez, J. R., Coleman, T. A., Dorshkind, K., McComas, W. A., Sarmiento, U. M., Rosen, C. A., and Narayanan, R. (1993) *Proc. Natl. Acad. Sci. U.S.A. 90*, 9901−9905.
22. Bielinska, A., Shivdasani, R., Zhang, L., and Nabel, G. (1990) *Science 250*, 997−1000.
23. Sharma, H. W., Perez, J. R., Higgins-Sochaski, K., Hsiao, R., and Narayanan, R. (1996) *Anticancer Res. 16*, 61−70.
24. Morishita, R., Sugimoto, T., Aoki, M., Kida, I., Tomita, N., Moriguchi, A., Maeda, K., Sawa, Y., Kaneda, Y., Higaki, J., and Ogihara, T. (1997) *Nat. Med. (N.Y.) 3*, 894−99.
25. Chen, H., and Gold, L. (1994) *Biochemistry 33*, 8746−8756.
26. Jaeger, J., Turner, D., and Zuker, M. (1989) *Proc. Natl. Acad. Sci. U.S.A. 86*, 7706−7710.
27. Jaeger, J., Turner, D., and Zuker, M. (1990) *Methods Enzymol. 183*, 281−306.
28. Zuker, M. (1989) *Science 244*, 48−52.
29. Sambrook, J., Fritsch, E. F., and Maniatis, T. (1989) *Molecular Cloning: A Laboratory Manual*, 2nd ed., Cold Spring Harbor Laboratory Press, Cold Spring Harbor, NY.
30. Huang, Z., and Szostak, J. (1996) *Nucleic Acids Res. 24*, 4360−4361.
31. Rickwood, D., and Hames, B. (1982) *Gel Electrophoresis of Nucleic Acids*, IRL Press, Washington, D.C.
32. Coleman, T. A., Huddleston, K. A., Ruben, S. M., Rosen, C. A., and Gentz, R. (1997) *Prot. Expression Purif. 9*, 40−48.
33. Pieler, T., and Theunissen, O. (1993) *Trends Biol. Sci. 18*, 226−230.
34. Rivera-Pomar, R., Niessing, D., Schmidt-Ott, U., Gehring, W. J., and Jackle, H. (1996) *Nature 379*, 746−749.
35. Dubnau, J., and Struhl, G. (1996) *Nature 379*, 694−699.
36. Baeuerle, P. A., and Baltimore, D. (1996) *Cell 87*, 13−20.
37. Nabel, G., and Baltimore, D. (1987) *Nature 326*, 711−713.
38. Makarov, S., Johnston, W., Olsen, J., Watson, J., Mondal, K., Rinehart, C., and Haskill, J. (1997) *Gene Ther. 4*, 846−852.

BI982515X